Smart Structures and Systems, *Vol. 27, No. 5 (2021) 795-801*
DOI: https://doi.org/10.12989/sss.2021.27.5.795

Experimental study on the optimized design of butterfly-shaped dampers

Jong Wan Hu [1,2a], Young Wook Cha [1,3b], Alireza Farzampour [4c], Nadia M. Mirzai [5d] and Iman Mansouri*[6,7]

[1] *Department of Civil and Environmental Engineering, Incheon National University, 22012 Incheon, South Korea*
[2] *Incheon Disaster Prevention Research Center, Incheon National University, Incheon, South Korea*
[3] *Korea Authority of Land & Infrastructure Safety, Jinju, South Korea*
[4] *Department of Civil and Environmental Engineering, Virginia Tech, Blacksburg, United States*
[5] *Department of Architectural Engineering, Inha University, 22212 Incheon, South Korea*
[6] *Department of Civil Engineering, Birjand University of Technology, 97175-569 Birjand, Iran*
[7] *Institute of Research and Development, Duy Tan University, Da Nang 550000, Vietnam*

(*Received May 30, 2020, Revised January 4, 2021, Accepted January 18, 2021*)

Abstract. Structural fuses are manufactured from oriented steel plates for use in seismic protective systems to withstand significant lateral shear loads. These systems are designed and detailed for concentrating the damage and excessive inelastic deformations in the desired location along the length of the fuse to prevent the crack propagation and structural issues for the surrounding elements. Among a number of structural systems with engineered - cut-outs, a recently developed butterfly-shaped structural fuses are proposed to better align the bending strength along the length of the fuse with the demand moment, enhancing controlled yielding features over the brittle behavior. Previously, the design methodologies were developed purely based on the flexural stresses' or shear stresses' behavior leading to underestimate or overestimate the structural capacity of the fuses. The aim of this study is to optimize the design methodologies for commonly used butterfly-shaped dampers through experimental investigations considering the stresses are not uniformly distributed stresses along the length of the fuse system. The effect of shear and flexural stresses on the behavior of butterfly-shaped are initially formulated based on the Von-Mises criterion, and the optimized geometry is specified. Subsequently, experimental tests are developed for evaluating the optimized design concepts for butterfly-shaped dampers considering the uniform stress distribution and efficient use of steel. It is shown that butterfly-shaped dampers are capable of full cyclic hysteric behavior without any major signs of strength or stiffness degradations.

Keywords: structural fuses; shear and flexural stresses; seismic damper; Von-Mises criteria; optimization

1. Introduction

The structures around the world are designed and constructed to prevent and postpone significant damages and collapse under hazard conditions. One of the practical solutions for designing resilient systems is to implement the structural fuses to concentrate damages within the desired location over a structural system (Farahi Shahri and Mousavi 2018, Farzampour *et al*. 2019b, c, Liu *et al*. 2015, Martínez-Rueda 2002, Mirzai *et al*. 2018, 2020a, b, 2021, Mirzai and Hu 2019, Nuzzo et al. 2018), and protect the surrounding parts from severe damages and then be replaceable after any events (Ahmadie Amiri *et al*. 2018, Eldin *et al*. 2018, Kim and Shin 2017, Shad *et al*. 2018, Zhan *et al*. 2017). The structural fuses have shown appropriate energy dissipation capability, ductility, high initial stiffness, and strategic plastic hinge formation to avoid crack propagations. Typically, the steel structural fuses consist of plates with engineered cut-outs yielded as subjected to shear loading conditions. Among various shapes and sizes studied in previous studies, the butterfly-haped shear fuses shown in Figs. 1 and 2 are used due to having a number of advantages over the rest of the structural fuse systems, and be used as an appropriate substitute for conventional EBF systems. The application of butterfly shaped dampers, geometry and the typical imposed loading are shown on Fig1.a, Fig.1b and Fig1.c, respectively. The reduction of seismic secondary effects, fewer disturbances caused by earthquakes, high energy dissipation, and efficient use of steel in the space-constrained area are previously reported for structural fuses (Luth *et al*. 2008, Farzampour and Eatherton 2018b, Esteghamati and Farzampour 2020, Zaker Esteghamati and Farzampour 2020). The yielding mechanism occurred along the length of the fuses, and prevention of the brittle limit states should be considered for enhancing the fuse resistance against the lateral loading and desired performance (Ke and Yam 2016, Sun *et al*. 2017). Recently, several applications of these systems are under process for use in high-rises buildings (as it shown in Fig. 2, in the USC School of Cinema). It is noted that there are several other systems used to reduce the seismic vulnerability of the

*Corresponding author, Associate Professor,
E-mail: mansouri@birjandut.ac.ir
[a] Ph.D.
[b] Ph.D. Candidate
[c] Ph.D.
[d] Ph.D.

ISSN: 1738-1584 (Print), 1738-1991 (Online)

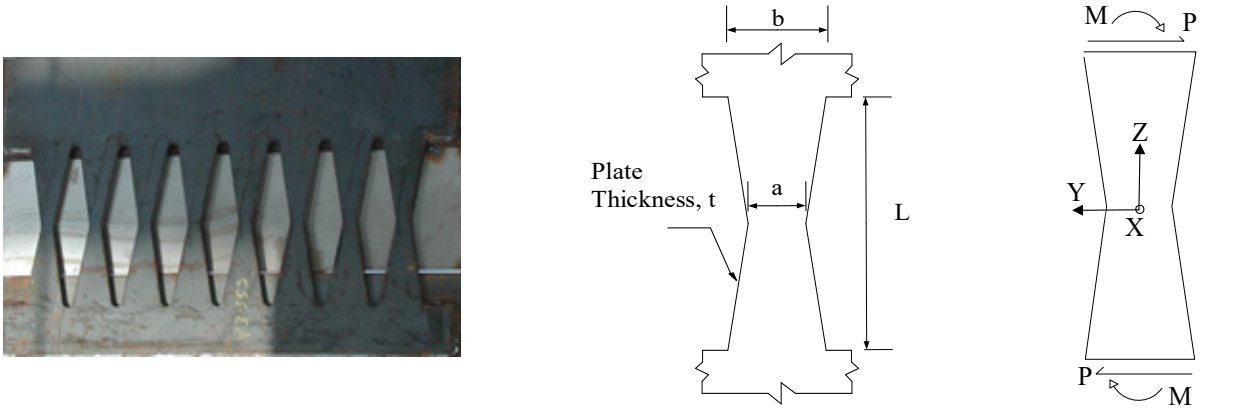

(a) Butterfly fuse plate (Luth *et al*. 2008) (b) Geometry (c) Loading condition

Fig. 1 The butterfly shape fuse (Farzampour *et al*. 2019a)

Fig. 2 The implementation of the butterfly-shaped fuses in USC School of Cinema (Luth *et al*. 2008)

structures. Buckling resistant braces are typically used to prevent the degradation of the stiffness and strength and obtain more stable hysteretic response, despite the high cost of construction and maintenance (Avci-Karatas 2019, Avci-Karatas and Celik 2014, Avci-Karatas *et al*. 2018, 2019, Mansouri *et al*. 2016). In addition, these systems similar to fuses could have advances such as replacement following an earthquake, easy fabrication with relatively low cost, simple details, which is useful for various retrofitting purposes.

To align the moment capacity with the shape of the moment demand diagram, various sectional geometries are previously investigated (e.g., straight dampers, butterfly-shaped) leading to efficient use of steel material along the length of the damper. Traditionally, a number of dampers were used in structural applications in in- and out-of-plane formats as added damping and stiffness or stiffness devices to be bent over the weak axis (Tsai *et al*. 1993, Whittaker *et al*. 1991). However, these links are able to work and bend over the major axis (in-plane bending) to develop uniform stress and larger in-plane stiffness. The planar use of the butterfly-shaped damper is previously investigated for various structural applications. The buckling limit states, load-carrying behavior, and energy dissipation capabilities of these dampers are addressed (Farzampour and Eatherton 2018a, b).

The substantial energy dissipating, ductility and large uniform yielding distribution are observed with the in-plane use of butterfly-shaped fuses, which made these dampers an appropriate option for use in in high-rise buildings leading to control drift response limitation and reducing the demands on the framing members (Hitaka and Matsui 2006, Kim *et al*. 2018, Luth *et al*. 2008). The previous design methodologies for majority of dampers are based on the flexural limit states underestimating or overestimating the dampers capacity against lateral forces. Numerous studies have shown that the stresses are not uniformly distributed along the length of the dampers (Lee *et al*. 2015, 2016a, b); hence, the design methodology and the effective implementation of the steel are in need of improvements.

In this study, both shear and flexure limit states are investigated under simultaneous shear and flexural stresses. The Von-Mises criterion is used to develop the upper limit for the total stresses imposed on the link. The flexural and shear stresses are developed based on the geometrical properties and mechanics of the shear fuses, which varies along the length of the link. The resulting stress function which includes flexural and shear stresses is optimized for having the plastic hinges far from the geometrical sharpness, and having the uniform stresses along the length of the damper.

The aim of this study is to propose an optimized design methodology to improve the behavior of the dampers for further uses in various supplications (Paslar *et al*. 2020a, b, Mansouri *et al*. 2020), especially the commonly used butterfly-shaped dampers while having the economical implementation of the steel. By implementation of the proposed methodology, the fundamental knowledge about the yielding behavior of the damping system is developed. In addition, the plastic mechanisms governing the strength and spread of the plasticity along the length of the dampers are investigated leading to seismic performance improvement of the shear fuses and reduce the damages due to earthquakes.

2. Methodology

The general analytical investigations of shear and flexure is explained and developed (Farzampour *et al*. 2019a, b, and c): both shear and flexure limit states are considered to be applied simultaneously. For this purpose, the Von-Mises criterion is initially implemented for setting the upper limit for the total stresses imposed on the link considering the flexural and shear behavior. The moment along the length $M(z)$ is formulated from the middle point as it is shown in Fig. 1, and the end moment M_0 is indicated in Eq. (1). The varying width is denoted by $w(z)$, and sectional inertia is defined with $I(z)$ of the link, which are shown in Eq. (2), and Eq. (3), respectively.

$$M(z) = \frac{2M_0 z}{L} \quad \text{and} \quad M_0 = PL/2 \tag{1}$$

$$w(z) = \frac{2(b-a)z}{L} + a \tag{2}$$

$$I(z) = \frac{1}{12} w(z)^3 t = \frac{1}{12}\left[\frac{2(b-a)}{L} z + a\right]^3 t \tag{3}$$

In which the geometrical parameters, a, b, L, t are defined in Fig. 1. Therefore, the flexural stress at a section is as shown in Eq. (4).

$$\sigma = \frac{M(z)}{I(z)} \frac{w(z)}{2} = \frac{Pz(w(z)/2 - y)}{\frac{1}{12}\left[\frac{2(b-a)}{L} z + a\right]^3 t} \tag{4}$$

Where the shear force is shown with P and it is applied to the end length of the butterfly-shaped link. Along the same lines shear stresses within the section (h) is defined based on the common mechanics of material equations, as it is shown in Fig. 3, and elaborated in Eq. (5).

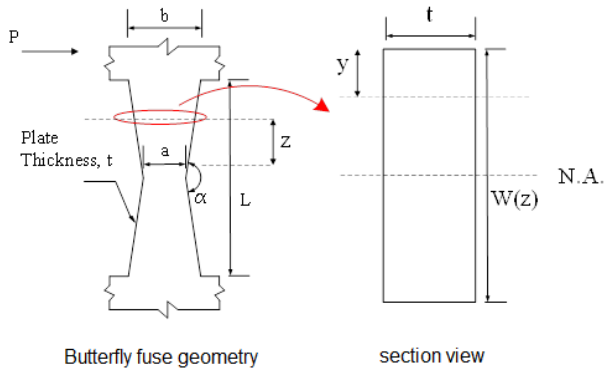

Fig. 3 The butterfly-shaped fuse

$$\eta = \frac{VQ}{It} = \frac{Pyt\left(\frac{w(z)}{2} - \frac{y}{2}\right)}{I(z)t} = \frac{Pyt\left(\left[\frac{2(b-a)}{L} z + a\right] - y\right)/2}{\frac{1}{12}\left[\frac{2(b-a)}{L} z + a\right]^3 t^2} \tag{5}$$

In addition, Von-Mises yielding criterion stress, which is shown in Eq. (6)

$$\sigma_y^2 = \frac{1}{2}[(\sigma_{11} - \sigma_{22})^2 + (\sigma_{22} - \sigma_{33})^2 + (\sigma_{33} - \sigma_{11})^2 + 6(\sigma_{23}^2 + \sigma_{31}^2 + \sigma_{12}^2)] \tag{6}$$

It is noted that the inelasticity is considered to be concentrated far from the ends and sharp edges to produce better resistance against the crack propagation and brittle modes of behavior. For this purpose, the term z should be equalized to $L/4$ recommending the farthest point away from the sharp edges to concentrate the plasticity; therefore, by substituting the $L/4$ for z, Eq. (7) is obtained as follows (Farzampour *et al*. 2019a).

$$\sigma_y = \sqrt{\left[\frac{1}{2}\left[\left(\frac{\frac{PL}{4}}{\frac{1}{12}\left[\frac{b+a}{2}\right]^3 t}\left(\left[\frac{b+a}{4}\right] - y\right)\right)^2 + 6\left(\frac{\frac{Py\left(\left[\frac{b+a}{2}\right]-y\right)}{2}}{\frac{1}{12}\left[\frac{b+a}{2}\right]^3 t}\right)^2\right]\right]} \tag{7}$$

The right-hand side of the Eq. (8) indicates stress state function indicated by $F(y)$, which combines the effect of shear with flexure stresses at a specific section located at $L/4$ from the midpoint of a BF link.

$$\mathrm{F}(y) = \left[\frac{1}{2}\left[\left(\frac{\frac{PL}{4}}{\frac{1}{12}\left[\frac{b+a}{2}\right]^3 t}\left(\left[\frac{b+a}{4}\right] - y\right)\right)^2 + 6\left(\frac{\frac{Py\left(\left[\frac{b+a}{2}\right]-y\right)}{2}}{\frac{1}{12}\left[\frac{b+a}{2}\right]^3 t}\right)^2\right]\right] \tag{8}$$

To have an efficient and economical fuse system, it is required to have the ductile yielding limit states occurred for all the points along the length of the link. The schematic stress state is shown in Fig. 4 to show a continuous function over the length of the link. For having constant state of stress over the length of the link, the difference between the minimum and the maximum critical stress points, as it is determined in Fig. 4, should be minimized indicating that the stress function reaches to a constant value along the length of the link.

To find the minimum and maximum values of the stress state function indicated in Eq. (8), the derivation of the stress function should be equalized to zero, which eventually would lead to three real roots as shown in Eq. (9). The three roots are as follows

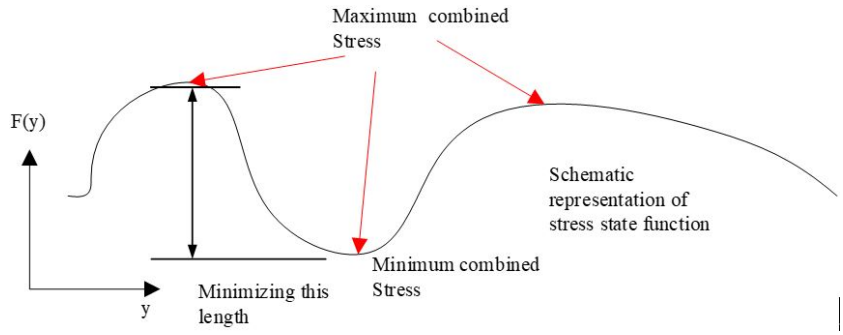

Fig. 4 Mathematical concepts for uniform stress (Farzampour *et al*. 2019a)

$$\begin{aligned} &I. \quad \frac{a}{4}+\frac{b}{4} \\ &II. \quad \frac{a}{4}+\frac{b}{4}-\frac{\sqrt{3}\left(\sqrt{3a^2+6ab+3b^2-L^2}\right)}{12} \\ &III. \quad \frac{a}{4}+\frac{b}{4}+\frac{\sqrt{3}\left(\sqrt{3a^2+6ab+3b^2-L^2}\right)}{12} \end{aligned} \tag{9}$$

Therefore, based on the developed concept mentioned within Fig. 4, the difference between the minimum and maximum values of the stress state function should approach zero to have the same stress state distribution for all the points along the length of the link, which is mathematically described as shown in Eq. (10).

$$\begin{aligned} &\mathrm{f}(II)-f(I)\approx 0 \\ &f(III)-f(II)\approx 0 \\ &\mathrm{f}(III)-f(I)\approx 0 \end{aligned} \tag{10}$$

By simplifying the set of equations proposed in Eq. (10), Eq. (11) is derived.

$$\mp\frac{6P^2(3a^2+6ab+3b^2-L^2)^2}{2t^2(a+b)^6}=0 \tag{11}$$

Eq. (11) is further simplified in Eq. (12). Therefore, the appropriate geometrical condition for having the inelasticity concentrated at the quarter points is derived according to Eq. (12).

$$3(a+b)^2=L^2 \tag{12}$$

The proposed geometry derived from the simultaneous effects of shear and flexural stresses for having the inelasticity located in quarter points in design is considered for further experimental evaluation in the following sections.

3. The experimental investigation

3.1 Test specimens

Three specimens were manufactured and tested in this study. The typical specimens, and the exact dimensions of the specimens are shown in Fig. 5 and tabulated in Table 1.

The chemical and mechanical properties of the used steel were per the Korean Industrial Standards (KS). The performance of metal dampers in vibration control is improved when the used metals have low yield stress (YS), low yield ratio (YR), and high ductility. SS400 Grade was selected as the damper construction material due to its low cost and availability in Korea.

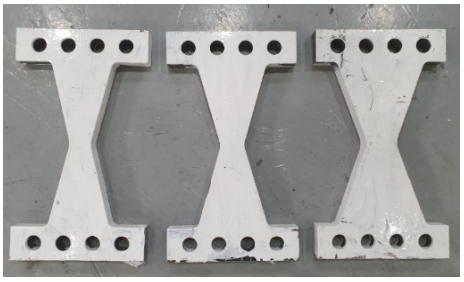

Fig. 5 Experimental butterfly-shaped fuse specimens

Table 1 Initial design values for uniform design concept

a (m)	b (m)	L (m)	t (m)
0.14	0.43	1.00	0.14
0.18	0.53	1.00	0.16
0.13	0.38	1.00	0.20

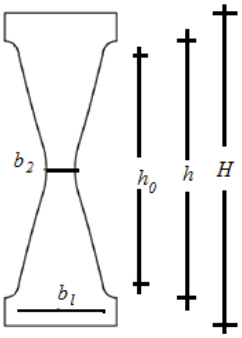

Fig. 6 The geometrical details of specimens (Ahmadie Amiri *et al*. 2018)

Three specimens sized according to Table 1 and Fig. 6 were tested. The specimens were designed to be connected with high-tensile bolts, without welding. Fig. 7 shows the configuration of the test setup.

The impact of hysteretic loadings was determined through an application of cyclic loading with incremental amplitudes. Fig. 8 shows the loading program. The design of the step amplitude (a_i) and the number of cycles was done to ensure that the range of the cumulative plastic

Fig. 7 The configuration of test setup

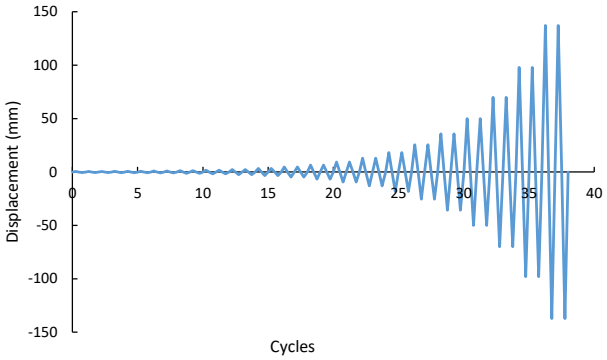

Fig. 8 The cyclic loading protocol with the loading rate ranged from 0.1 to 0.5 mm/s

deformation experienced by the specimens was sufficient (Farzampour *et al*. 2019). The equation, $a_{i+1} = 1.4\ a_i$, was used to determine the displacements in successive steps from step 1 to step 12. Increment of displacements after the 12th step was kept constant at 5.4 mm. The loading rate (v) ranged from 0.1 to 0.5 mm/s.

4. Experimental results and discussions

4.1 Hysteretic behavior and the deformed shapes

Fig. 9 shows the experimental and analytical force-displacement hysteresis curves for the specimens. From these figures, it can be concluded that all samples produced stable hysteresis curves with no sudden degradation of strength and stiffness. Specimens, whose h_0/b_1 ratios were high, formed butterfly-shaped hysteresis loops. Those with low h_0/b_1 ratios formed almost parallelogram-shaped hysteresis loops with high energy dissipation capacities. Decreasing the h_0/b_1 ratios through specimens S1 to S3 widened the hysteresis loops but reduced the displacements capacities. Fig. 10 displays the final deformed shape of the specimens and their failure spots.

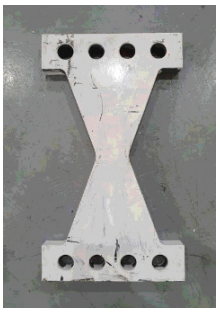

Fig. 10 The final deformed shape of the specimens and their failure spots

4.2 Structural parameters of the specimens

An idealized multi-linear force-displacement curve derived from monotonic backbone curves was used to determine the specimens' structural parameters. The backbone curves were obtained from each specimen's force-displacement hysteresis curve. The monotonic curves were idealized such that the initial and idealized areas under the monotonic curves were equal. Benavent-Climent developed a procedure in the year 2010 to derive backbone curves (Farzampour and Eatherton 2018b). The same procedure was used to obtain the backbone curves for these specimens. An example of the initial and idealized backbone curve for the specimen S1 is shown in Fig. 11.

The idealized multi-linear force-displacement curves and structural parameters for each specimen is obtained based on pushover curve from the cyclic backbone behavior. The backbone curves are obtained based on the specimen's force-displacement hysteresis curves. Subsequently, the monotonic curves are idealized in such a way that the area under the monotonic and cyclic curves are the same which is based on the utilization of the previous procedures (Farzampour and Eatherton 2018b). For example, the initial and idealized backbone curve for the specimen S1 is depicted in Fig. 10.

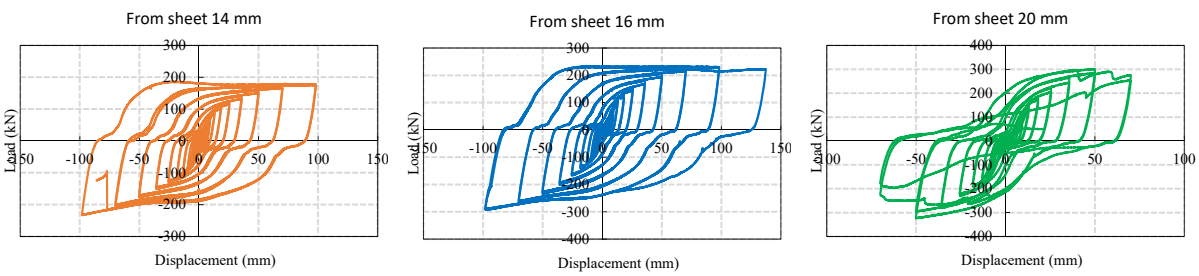

Fig. 9 Experimental results: load–displacement hysteresis loops

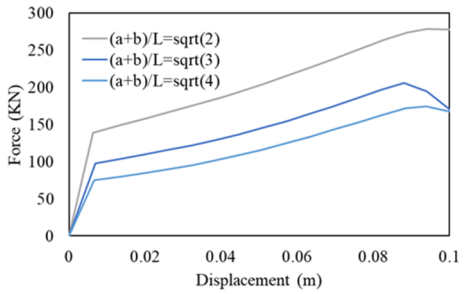

Fig. 11 Backbone curve of specimens

Table 2 Experimental results

N	P_y (kN)	δ_y (mm)	K_e (kN/mm)	P_m (kN)	δ_m (mm)	μ_c	E_D (kJ)
S1	185	65	2.8	210	97	1.49	60.4
S2	221	48	4.6	297	55	1.14	89.3
S3	297	27	11	330	38	1.40	67.5

The idealized backbone curves for the specimens were used to derive structural parameters such as the yield force (P_y), yield displacement (δ_y), initial elastic stiffness (K_e), second yield force (P_B). As well, the maximum force (P_{max}), maximum displacement (δ_{max}), Energy dissipation for the largest hysteresis (E_D) and the ductility capacity (μ_c) were derived from the force-displacement curves. These parameters are presented in Table 2.

Decreasing the h_0/b_1 ratio tends to reduce the number of curves in the idealized backbone graph for the specimens from three, as shown in Fig. 11 to two as the second and ultimate stiffness tends to merge. As well, P_y, K_e, P_B, P_{max}, and ED increase while δ_{max}, μ_c decrease. Specimens S1 and S3 failed before the anticipated displacements. However, ignoring these two specimens, it can be concluded that the specimens' displacement capacities vary from 22.15 mm to 125.5 mm.

5. Conclusions

To concentrate the damages and at a desired location within the structures, structural fuses are implemented. The implementation of the fuses has several advantages to reduce the seismic vulnerability of the structures. The systems are typically used to prevent the degradation of the stiffness and strength and obtain more stable hysteretic response. The use of structural fuses leads to further surrounding elements protection from high force demand and inelasticity. This study investigates the design methodology for general structural fuses under simultaneous effects of shear and flexural stresses. For this purpose, Butterfly-shaped fuses are optimized based on the yielding criterion and designing geometrical aspects are defined. Subsequently, several experimental specimens are developed to effectively compare and study the seismic behavior of the fuses. It is shown that butterfly-shaped dampers are capable of full cyclic hysteric behavior without any major signs of strength or stiffness degradation. In general, the dampers, designed in such a way that the brittle limit states are avoided, the energy mechanism, in those soft dampers are derived based on the shear deformations. The general deformations could be occurred due to shear and flexure mechanisms, which are also considered as the two typical, desirable modes of behavior. In addition, it is determined that the procedures elaborated in this study could be implemented for improving any general structural fuse shape considering simultaneous shear and flexural stresses.

Acknowledgments

This work was supported by Incheon National University Research Concentration Professors Grant in 2019.

References

Ahmadie Amiri, H., Najafabadi, E.P. and Estekanchi, H.E. (2018), "Experimental and analytical study of Block Slit Damper", *J. Constr. Steel Res.*, **141**, 167-178. https://doi.org/https://doi.org/10.1016/j.jcsr.2017.11.006

Avci-Karatas, C. (2019), "Prediction of ultimate load capacity of concrete-filled steel tube columns using multivariate adaptive regression splines (MARS)", *Steel Compos. Struct., Int. J.*, **33**(4), 583-594. https://doi.org/10.12989/scs.2019.33.4.583

Avci-Karatas, C. and Celik, O.C. (2014), "Cyclic testing of steel-core buckling-restrained braces (BRBs) having simple end details and infilled with high strength grout", *Proceedings of the NCEE 2014 - 10th U.S. National Conference on Earthquake Engineering: Frontiers of Earthquake Engineering*.

Avci-Karatas, C., Celik, O.C. and Yalcin, C. (2018), "Experimental investigation of aluminum alloy and steel core buckling restrained braces (BRBs)", *Int. J. Steel Struct.*, **18**(2), 650-673. https://doi.org/10.1007/s13296-018-0025-y

Avci-Karatas, C., Celik, O.C. and Ozmen Eruslu, S. (2019), "Modeling of buckling restrained braces (BRBs) using full-scale experimental data", *KSCE J. Civ. Eng.*, **23**(10), 4431-4444. https://doi.org/10.1007/s12205-019-2430-y

Eldin, M.N., Kim, J. and Kim, J. (2018), "Optimum distribution of steel slit-friction hybrid dampers based on life cycle cost", *Steel Compos. Struct., Int. J.*, **27**(5), 633-646. https://doi.org/10.12989/scs.2018.27.5.633

Esteghamati, M.Z. and Farzampour, A. (2020a), "Probabilistic seismic performance and loss evaluation of a multi-story steel building equipped with butterfly-shaped fuses", *J. Cons. Steel Res.*, **172**, 106187. https://doi.org/10.1016/j.jcsr.2020.106187

Farahi Shahri, S. and Mousavi, S.R. (2018), "Seismic behavior of beam-to-column connections with elliptic slit dampers", *Steel Compos. Struct., Int. J.*, **26**(3), 289-301. https://doi.org/10.12989/scs.2018.26.3.289

Farzampour, A. and Eatherton, M.R. (2018a), "Investigating limit states for butterfly-shaped and straight shear links", *Proceedings of the 16th European Conference on Earthquake Engineering, 16ECEE*, Thessaloniki, Greece.

Farzampour, A. and Eatherton, M.R. (2018b). "Parametric study on butterfly-shaped shear links with various geometries", *Proceedings of the 11th National Conference on Earthquake Engineering, 11NCEE*, Los Angeles, USA.

Farzampour, A., Eatherton, M.R., Mansouri, I. and Hu, J.W. (2019a), "Effect of flexural and shear stresses simultaneously for optimized design of butterfly-shaped dampers:

Computational study", *Smart Struct. Syst., Int. J.*, **23**(4), 329-335. https://doi.org/10.12989/sss.2019.23.4.329

Farzampour, A., Khatibinia, M. and Mansouri, I. (2019b), "Shape optimization of butterfly-shaped shear links using Grey Wolf algorithm", *Ing. Sismica*, **36**(1), 27-41.

Farzampour, A., Mansouri, I. and Dehghani, H. (2019c), "Incremental dynamic analysis for estimating seismic performance of multi-story buildings with butterfly-shaped structural dampers", *Build.*, **9**(4), p. 78. https://doi.org/10.3390/buildings9040078

Hitaka, T. and Matsui, C. (2006), "Seismic performance of Steel Shear Wall with Slits integrated with multi story composite moment frame", *Proceedings of the 5th International Conference on Behaviour of Steel Structures in Seismic Areas, STESSA 2006*, Yokohama, Japan, 241-246.

Ke, K. and Yam, M.C.H. (2016), "Energy-factor-based damage-control evaluation of steel MRF systems with fuses", *Steel Compos. Struct., Int. J.*, **22**(3), 589-611. https://doi.org/10.12989/scs.2016.22.3.589

Kim, J. and Shin, H. (2017), "Seismic loss assessment of a structure retrofitted with slit-friction hybrid dampers", *Eng. Struct.*, **130**, 336-350. https://doi.org/https://doi.org/10.1016/j.engstruct.2016.10.052

Kim, J., Kim, M. and Eldin, M.N. (2018), "Optimal distribution of steel plate slit dampers for seismic retrofit of structures", *Steel Compos. Struct., Int. J.*, **25**(4), 473-484. https://doi.org/10.12989/scs.2017.25.4.473

Lee, C.H., Ju, Y.K., Min, J.K., Lho, S.H. and Kim, S.D. (2015), "Non-uniform steel strip dampers subjected to cyclic loadings", *Eng. Struct.*, **99**, 192-204. https://doi.org/10.1016/j.engstruct.2015.04.052

Lee, C.H., Kim, J., Kim, D.H., Ryu, J. and Ju, Y.K. (2016a), "Numerical and experimental analysis of combined behavior of shear-type friction damper and non-uniform strip damper for multi-level seismic protection", *Eng. Struct.*, **114**, 75-92. https://doi.org/10.1016/j.engstruct.2016.02.007

Lee, C.H., Lho, S.H., Kim, D.H., Oh, J. and Ju, Y.K. (2016b), "Hourglass-shaped strip damper subjected to monotonic and cyclic loadings", *Eng. Struct.*, **119**, 122-134. https://doi.org/10.1016/j.engstruct.2016.04.019

Liu, L., Lei, Y. and He, M. (2015), "Locating and identifying model-free structural nonlinearities and systems using incomplete measured structural responses", *Smart Struct. Syst., Int. J.*, **15**(2), 409-424. https://doi.org/10.12989/sss.2015.15.2.409

Luth, G., Krawinkler, H. and McDonald, B. (2008), "USC School of Cinema: An example of reparable performance based design", *Proceedings of the 77th Annual Structural Engineers Association of California* (*SEAOC*) *Convention*, Structural Engineers Association of Southern California, Fulllerton, CA, USA.

Mansouri, I., Safa, M., Ibrahim, Z., Kisi, O., Tahir, M.M., Baharom, S. and Azimi, M. (2016), "Strength prediction of rotary brace damper using MLR and MARS", *Struct. Eng. Mech., Int. J.*, **60**(3), 471-488. https://doi.org/10.12989/sem.2016.60.3.471

Mansouri, I., Arabzadeh, A., Farzampour, A. and Hu, J.W. (2020), "Seismic behavior investigation of the steel multi-story moment frames with steel plate shear walls", *Steel Compos. Struct., Int. J.*, **37**(1), 91-98. http://doi.org/10.12989/scs.2020.37.1.091

Martínez-Rueda, J.E. (2002), "On the evolution of energy dissipation devices for seismic design", *Earthq. Spectra*, **18**(2), 309-346. https://doi.org/10.1193/1.1494434

Mirzai, N.M. and Hu, J.W. (2019), "Pilot study for investigating the inelastic response of a new axial smart damper combined with friction devices", *Steel Compos. Struct., Int. J.*, **32**(3), 373-388. https://doi.org/10.12989/scs.2019.32.3.373

Mirzai, N.M., Attarnejad, R. and Hu, J.W. (2018), "Enhancing the seismic performance of EBFs with vertical shear link using a new self-centering damper", *Ing. Sismica*, **35**(4), 57-76.

Mirzai, N.M., Attarnejad, R. and Hu, J.W. (2020a), "Analytical investigation of the behavior of a new smart recentering shear damper under cyclic loading", *J. Intell. Mater. Syst. Struct.*, **31**(4), 550-569. https://doi.org/10.1177/1045389X19888786

Mirzai, N.M., Attarnejad, R. and Hu, J.W. (2020b), "Experimental investigation of smart shear dampers with re-centering and friction devices", *J. Build. Eng.*, 102018. https://doi.org/https://doi.org/10.1016/j.jobe.2020.102018

Mirzai, N.M., Cho, H.M. and Hu, J.W. (2021), "Experimental study of new axial recentering dampers equipped with shape memory alloy plates", *Struct. Control Health Monit.*, **28**(3). https://doi.org/10.1002/stc.2680

Nuzzo, I., Losanno, D., Caterino, N., Serino, G. and Bozzo Rotondo, L.M. (2018), "Experimental and analytical characterization of steel shear links for seismic energy dissipation", *Eng. Struct.*, **172**, 405-418. https://doi.org/https://doi.org/10.1016/j.engstruct.2018.06.005

Shad, H., Bin Adnan, A., Vafaei, M., Behbahani, H.P. and Oladimeji, A.M. (2018), "Experimental study on TLDs equipped with an upper mounted baffle", *Smart Struct. Syst., Int. J.*, **21**(1), 37-51. https://doi.org/10.12989/sss.2018.21.1.037

Sun, B., Wang, M. and Gao, L. (2017), "Design principles for stiffness-tandem energy dissipation coupling beam", *Smart Struct. Syst., Int. J.*, **20**(1), 53-60. https://doi.org/10.12989/sss.2017.20.1.053

Tsai, K.-C., Chen, H.-W., Hong, C.-P. and Su, Y.-F. (1993), "Design of steel triangular plate energy absorbers for seismic-resistant construction", *Earthq. Spectra*, **9**(3), 505-528. https://doi.org/10.1193/1.1585727

Whittaker, A.S., Bertero, V.V., Thompson, C.L. and Alonso, L.J. (1991), "Seismic testing of steel plate energy dissipation devices", *Earthq. Spectra*, **7**(4), 563-604. https://doi.org/10.1193/1.1585644

Zaker Esteghamati, M. and Farzampour, A. (2020b), "Probabilistic seismic assessment of a mid-rise eccentrically braced steel frame equipped with butterfly-shaped dampers", *Proceedings of the 17th World Conference on Earthquake Engineering*, Sendai, Japan, September.

Zhan, M., Wang, S., Yang, T., Liu, Y. and Yu, B. (2017), "Optimum design and vibration control of a space structure with the hybrid semi-active control devices", *Smart Struct. Syst., Int. J.*, **19**(4), 341-350. https://doi.org/10.12989/sss.2017.19.4.341

CC